HHS Public Access

Author manuscript

Cell Rep. Author manuscript; available in PMC 2017 September 06.

Published in final edited form as:

Cell Rep. 2016 September 6; 16(10): 2763–2776. doi:10.1016/j.celrep.2016.08.017.

Inhibiting the mitochondrial calcium uniporter during development impairs memory in adult *Drosophila*

Ilaria Drago and **Ronald L. Davis***

Department of Neuroscience, The Scripps Research Institute Florida, Jupiter, FL 33458, USA

Summary

The uptake of cytoplasmic calcium into mitochondria is critical for a variety of physiological processes, including calcium buffering, metabolism and cell survival. We demonstrate here that inhibiting the mitochondrial calcium uniporter in the *Drosophila* mushroom body neurons (MBn) – a brain region critical for olfactory memory formation – causes memory impairment without altering the capacity to learn. Inhibiting uniporter activity only during pupation impaired adult memory, whereas the same inhibition during adulthood was without effect. The behavioral impairment was associated with structural defects in MBn, including a decrease in synaptic vesicles and an increased length in the axons of the αβ MBn. Our results reveal an *in vivo* developmental role for the mitochondrial uniporter complex in establishing the necessary structural and functional neuronal substrates for normal memory formation in the adult organism.

Graphical Abstract

*Correspondence: rdavis@scripps.edu.

Author Contributions

I.D. and R.L.D. designed the experiments and wrote the manuscript. I.D. performed and analyzed experiments.

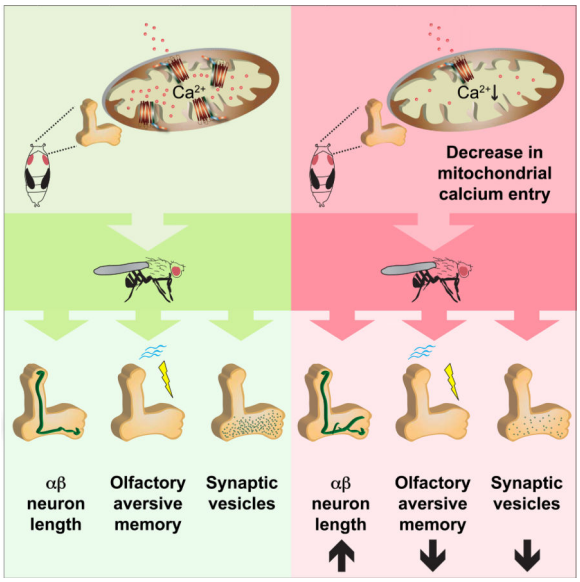

Introduction

The mitochondrion is a pivotal player in orchestrating the complexities of cellular calcium signaling (Rizzuto et al., 2012). Decades of research have demonstrated that mitochondrial calcium handling impacts diverse aspects of cellular physiology including metabolism, cell survival and autophagy (Rizzuto et al., 2012). The recent identification of proteins involved in Mitochondrial Calcium Entry (MCE) has significantly advanced our knowledge of cytoplasmic/mitochondrial calcium interactions and offered molecular tools to explore more deeply the physiological roles of MCE (Kamer and Mootha, 2015).

MCE is mediated by a macromolecular complex composed by the pore forming subunit, the Mitochondrial Calcium Uniporter (MCU), and several regulatory subunits including MICU1, MICU2, and EMRE (Baughman et al., 2011; De Stefani et al., 2011; Perocchi et al., 2010; Plovanich et al., 2013; Sancak et al., 2013) (Figure 1A). MCU is a highly conserved protein bearing two transmembrane domains connected by a loop facing the intermembrane space (Baughman et al., 2011; De Stefani et al., 2011). The calcium selective pore of the complex is likely formed as a pentamer of MCU subunits (Oxenoid et al., 2016). The regulatory subunit MICU1 resides in the mitochondrial intermembrane space (Csordas et al., 2013). MICU1 and its paralog MICU2 (Plovanich et al., 2013) together detect changes in cytoplasmic calcium and modulate the activity of MCU (Kamer and Mootha, 2014; Patron et al., 2014), while the inner mitochondrial membrane protein EMRE is required for the assembly of the uniporter complex (Sancak et al., 2013).

A fascinating aspect surrounding MCE is the observation that human patients carrying loss-of-function mutations in MICU1 exhibit learning disability, along with skeletal muscle myopathy and movement disorders (Lewis-Smith et al., 2016; Logan et al., 2014). Moreover, deficits in cognition are associated with many mitochondrial protein mutations (Finsterer, 2012), and many neurodegenerative disorders have associated mitochondrial defects (Schon and Przedborski, 2011). Experiments performed in rhesus monkeys demonstrated that the

number of normal, oblong-shaped mitochondria (as opposed to ‘donut-shaped’ malformed ones) directly correlates with synapse size and working memory test scores, thus suggesting that mitochondrial functions are important for learning and memory processes (Hara et al., 2014, 2016). There are, however, no studies investigating the hypothesis that MCE is linked to cognitive function. MCU knockout mice on an outbred strain display only a very mild muscle phenotype, but embryonic lethality when crossed into a C57BL/6 inbred line (Murphy et al., 2014; Pan et al., 2013). Learning and memory tests on these animals have not yet been reported.

Drosophila melanogaster is an invaluable model organism to discover new connections between genes involved in MCE and cellular and behavioral functions due to the ease of performing large forward genetic screens and the tools to control transgene expression in both time and space. In a large behavioral screen of olfactory memory using flies expressing individual RNAi’s in all neurons, Walkinshaw et al. (2015) identified hundreds of new genes whose disruption impaired or enhanced memory formation. Two components of the mitochondrial uniporter complex, MCU and MICU1, were identified among those that impaired memory when silenced.

This prompted us to test the hypothesis that MCE regulates memory formation and probe a mechanistic understanding for its role. We found that normal MCE is required in the mushroom body neurons (MBn) – a primary neuronal assembly of the olfactory nervous system – for normal Intermediate-Term Memory (ITM).

Surprisingly, although the behavioral phenotype was assayed in adult animals, the requirement for normal MCE occurred during the developmental stage of pupation. Moreover, the ITM deficit was not associated with a detectable learning deficit, as one might expect from a developmental genetic insult. In addition, we found evidence that inhibiting MCE in MBn causes a decrease in synaptic vesicle content and an increase in axonal length and field volume. Thus, normal MCE establishes, during development, a neuronal structural and/or functional competence for supporting adult memory.

Results

MCU expression and function in MBn is necessary for intermediate-term memory but not learning

The *Drosophila* gene *CG1876* is the homolog of mammalian MCU and its protein product localizes to mitochondria (Lye et al., 2014). *CG18769* was first identified as a candidate gene in a pan-neuronal RNAi screen aimed at discovering new genes that are critical for memory formation (Walkinshaw et al., 2015). When silenced, it impaired ITM, tested 3 hr after conditioning. Based on these results, we hypothesized that MCE is critical for memory formation.

To extend this observation, we silenced MCU by crossing the *CG18769*-specific *UAS-RNAi* line (v110781) with *GAL4;UAS-dcr2* fly lines representing different neuronal subpopulations of the *Drosophila* olfactory system (Figure 1B). Line 60100, that bears the same, but empty, docking sites used to insert *MCU RNAi* in v110781 flies was crossed to

the same battery of *GAL4>UAS-dcr2* lines as the control. Silencing MCU using the pan-neuronal driver *nSyb-GAL4* produced memory impairment when tested 3 hr after training (Figure 1C). The MBn-preferential drivers, *238y-* and *R13F02-GAL4*, were the only drivers that reproduced the 3 hr memory impairment observed with pan-neuronal MCU silencing. These results map MCU function to MBn (Figure 1C). Ubiquitous expression of *MCU RNAi* produced lethality. Crosses of either *Actin-GAL4/CyO* or *Tubulin-GAL4/TM3* to homozygous *UAS-MCU RNAi* flies produced only progeny carrying the balancer chromosome.

We focused experiments at this point using *R13F02-GAL4* as a driver, since it displays strong MBn expression with extremely limited expression in other populations of neurons (http://flweb.janelia.org/cgi-bin/view_flew_imagery.cgi?line=R13F02). We tested the *UAS-MCU RNAi* insertion alone and found it performs equivalently to *R13F02-GAL4*, with memory impairment occurring only upon combining the driver and *UAS-RNAi* transgene (Figure 1D).

We measured memory decay by training flies and testing their memory at different time points after conditioning (Figure 1E). While the immediate memory (3 min) of control and silenced flies was not significantly different, MCU silencing produced an ITM impairment, demonstrated by the significant decrease in 1 and 3 hr memory (Figure 1E). This deficit was not attributable to an impaired ability of MCU silenced flies to perceive the odors and the shock used during the training protocol as measured by standard avoidance tests (Figure S1A). To test the possibility that MCU silencing produces a learning impairment that is too subtle to be revealed by the standard training protocol, which employs odor presentation coupled with 12 shock pulses at 90V, we trained flies using fewer shocks (Figure 1F) or a lower voltage (Figure S1H). No significant difference was observed between control and MCU silenced flies, confirming that MCU function is required in the MBn for ITM but not for olfactory learning.

ITM is composed of two distinct types of memory – Anesthesia Sensitive Memory (ASM) and Anesthesia Resistant Memory (ARM; Guven-Ozkan and Davis, 2014). While ASM is eliminated by a cold shock performed between training and testing, ARM represents a consolidated form of memory that remains unaffected by this insult.

To better characterize the decrease in ITM observed upon MCU silencing, we eliminated the ASM portion of ITM by performing a cold shock 2 hr after training. Three hour memory in MCU silenced flies after cold shock was statistically lower than the cold shocked controls, revealing that MCU expression in MBn neurons is required for ARM (Figure 1G). A second assay for ARM is to measure memory at 24 hr after 5 consecutive cycles of training without any rest between cycles. Such massed conditioning produces ARM that persists more than a day but is independent of new protein synthesis. After 5X massed training, MCU silenced flies exhibited depressed 24 hr memory compared to the controls, confirming that MCU function supports ARM (Figure 1H)

We considered the possibility that the memory impairment occurred through off-target effects of the RNAi transgene. We thus searched for an independent method to confirm the

hypothesis that MCU is required in MBn for normal ITM. The substitution of two negatively charged amino acids in the DIME domain of MCU creates a dominant negative form of the channel (Baughman et al., 2011; De Stefani et al., 2011) (Figure 1A). We therefore generated flies with the insertion of *UAS-MCU*^{D260Q,E263Q} carrying a FLAG epitope. We verified the mitochondrial localization of MCU^{D260Q,E263Q} by driving its expression in MBn together with a mitochondrial targeted GFP (mito-GFP). The punctate expression of the anti-FLAG epitope (Figure 2A) was coincident with mito-GFP (Figure 2C) as detected with anti-GFP immunohistochemistry (Figure 2B).

The expression of *MCU*^{D260Q,E263Q} in MBn did not produce any impairment in immediate memory (Figure 2D) but caused a significant decrease in 3 hr memory compared to the GAL4-only and UAS-only controls (Figure 2E). The same conclusion was reached upon testing a second and independent MCU^{D260Q,E263Q} line with expression in MBn (Figure 2F). As already observed with MCU silencing, MCU^{D260Q,E263Q} expression in MBn did not cause a learning impairment, even when flies were subjected to a sub-maximal training protocol (Figure 2G). Finally, we verified that *MCU*^{D260Q,E263Q} expression did not alter odors or shock avoidance (Figure S1D). Collectively, these results demonstrate that MCU expression and function are required in MBn to support ITM, but not learning.

Impairing MCU function in MBn decreases MCE

The results above suggested that the impairment of ITM occurring with genetic insults to MCU function were due to decreased MCE. To confirm this we generated flies expressing a calcium reporter targeted to the mitochondrial matrix. Upon crossing *UAS-4mtGCaMP3* flies with a MBn driver, we observed a punctate pattern of fluorescence in the tip of the MBn vertical lobe that was characteristic of mitochondria (Figure 3A). We then tested the ability of the reporter to measure calcium changes by stimulating isolated brains expressing 4mtGCaMP3 with KCl. This challenge produced increased fluorescence with increasing KCl concentrations that reached a threshold at 50 mM, consistent with the interpretation that KCl treatment increased cytoplasmic calcium that in turn activated MCE (Figure 3B).

To confirm the expected localization of the 4mtGCaMP3 reporter to the mitochondrial matrix, we pre-incubated brains with FCCP, an ionophore that dissipates the mitochondrial potential and thus eliminates the driving force for mitochondrial, but not cytoplasmic, calcium entry. FCCP pre-treatment completely abolished the increase of 4mtGCaMP3 signal upon stimulation with KCl, confirming that the reporter properly localizes in the mitochondrial matrix (Figure 3C).

We then asked whether the genetic insults to MCU function that cause a decrease in ITM produce a decrease in MCE. We compared the mitochondrial calcium peak response upon KCl stimulation in control and MCU silenced brains (Figure 3D). MCE with MCU silencing was 18%±11% of the control response, normalized to 100%, thus demonstrating that *MCU RNAi* effectively impaired MCE. In MCU^{D260Q,E263Q} expressing brains, the response upon KCl stimulation was 46%±11% of the control (Figure 3E). These experiments demonstrate that the genetic insults using *UAS-MCU RNAi* or *UAS-MCU*^{D260Q,E263Q} expression dramatically decreased MCE that likely translate to impaired ITM.

Silencing MICU1 in MBn recapitulates the memory impairment caused by silencing MCU

Another component of the uniporter complex that was identified as a hit in the original RNAi screen was *CG4495* (Walkinshaw et al., 2015), the *Drosophila* homolog of MICU1. To further characterize MICU1's role in learning and memory, we silenced MICU1 in MBn. While 3 min memory in MICU1-silenced flies was indistinguishable from the control (Figure 4A), 3 hr memory was impaired (Figure 4B). MICU1 silencing failed to reveal a learning defect as assayed with sub-maximal training protocols (Figure 4C). Moreover, the memory decrease was not attributable to an odor or shock avoidance defect (Figure S1E). The memory decay curve of MICU1-silenced flies revealed an ITM defect (Figure 4D), while cold shock (Figure 4E) and massed training experiments (Figure 4F) showed that MICU1 is required for ARM, similar to that observed with MCU silencing. Like our results using *UAS-MCU RNAi*, silencing MICU1 using the ubiquitous drivers *Actin-GAL4/CyO* or *Tubulin-GAL4/TM3* failed to produce progeny without a balancer chromosome. We then measured the effect of *MICU1 RNAi* on MCE. Upon KCl stimulation, flies with MICU1 silenced in the MBn showed a mitochondrial calcium increase that was 70%±6% of the control (Figure 4G).

The results of these experiments silencing MICU1 in the MBn along with the results from two genetic insults directed at MCU provide compelling evidence that MCE impairment is associated with a memory deficit at intermediate times after conditioning but with no detectable difference in learning.

MCE in MBn is required during development to support ITM in adult flies

The simplest model derived from the above results that incorporates general knowledge about calcium signaling in physiological events was that MCE might underlie ITM mediated by MBn in an acute way at the time of conditioning and testing of adult flies. Since the genetic insults used were also present during the development of the organism, the less likely model was that MCE participated in some process during the development of the MBn that was required for the competence of these neurons to support ITM.

We took advantage of the TARGET system (McGuire et al., 2003) to distinguish between these two alternatives. TARGET employs the constitutive expression of the temperature sensitive GAL4 inhibitor GAL80 ($GAL80^{ts}$) to suppress GAL4 function at 18C. Shifting flies from 18C to 30C destabilizes $GAL80^{ts}$ and thus allows GAL4 to drive the expression of *UAS* insertions. We tested the 3 hr memory of flies carrying the *tub-GAL80*^{ts} insertion in which *MCU RNAi, MICU1 RNAi* or $MCU^{D260Q,E263Q}$ were expressed in MBn only during adulthood (18C-30C condition) or development (30C-18C condition), with temperature shifts occurring right after adult eclosion. As a negative control, we employed flies maintained at 18C, while flies maintained at 30C were used as the positive control (Figure 5A).

The results from this experiment produced the stunning conclusion that MCE is required during development and not during adulthood for normal ITM (Figure 5A). The temperature shift condition that reproduced the ITM impairment observed earlier due to MCE inhibition both during development and adulthood was 30C-18C, demonstrating that an efficient MCE

before adult eclosion is necessary to support ITM in adult flies. Shifting flies from 18C to 30C after eclosion to impair MCE during adulthood was without effect on memory.

To further delimit MCE requirement during development, we performed TARGET experiments restricting MCU silencing to more precise developmental stages. We synchronized the development of broods of flies by allowing parents an egg-laying time window of 6 hr. While MCU silencing until late third instar failed to alter 3 hr memory in adult flies, silencing from the late third instar to eclosion produced a significant decrease in 3 hr memory (Figure 5B). We then shifted flies after puparium formation. Mushroom bodies undergo a profound reorganization during pupation (Lee et al., 1999). Flies in which MCU was silenced in MBn from egg laying to puparium formation exhibited unimpaired 3 hr memory (Figure 5C). In contrast, silencing MCU starting after pupariation was sufficient to produce an ITM defect in adult flies (Figure 5C). These results map the requirement for MCE function to pupation.

Normal MCE in the αβ and γ MBn is required for normal ITM

The MBn in adult flies are classed into three major structural types whose axons project into brain neuropil areas termed the αβ, α’ β’, and γ lobes (Guven-Ozkan and Davis, 2014). As detailed above, MCE function in the MBn for ITM maps to pupation, a stage during which the already formed γ MBn axons are being pruned and the αβ MBn are born (Lee et al., 1999). To determine whether MCE is required specifically in one of the three classes of MBn, we silenced MCU with a panel of MBn-specific *GAL4* drivers (Figure 6A). None of the tested MBn subclass-specific drivers reproduced the 3 hr memory decrease observed with MCU silencing using a pan-MBn driver. This might be due to at least three different reasons. First, it may be that the drivers tested do not have the necessary potency. Second, the drivers tested may not be expressed during the required pupal stage necessary to see the effect. Third, the ITM memory phenotype observed with pan-MBn drivers may be due to the composite expression in more than one class of MBn.

We reasoned that the latter possibility was most likely and tested this idea using drivers that express *GAL4* in two of the three major MBn classes. We failed to see a significant decrease in adult ITM upon driving the expression of *UAS-MCU* with *NP1131-GAL4*, an element promoting expression in both α’β’ and γ MBn, or by driving expression with a combination of α’β’ and αβ-specific MBn drivers (*c305a-* and *c739-GAL4*) (Figure 6A). In contrast, we observed a significant decrease in ITM using *201y-GAL4* and *R25H11-GAL4*, elements that promote expression in both αβ and γ MBn. We also found the same aforementioned developmental requirement for this pair of MBn types using *201y-GAL4* in temperature shift TARGET experiments (Figure S2A). We examined the expression pattern of these *GAL4* elements along with the pan-MBn driver *R13F02-GAL4* by imaging the mCD8::GFP reporter during the phenocritical period of pupation (Figure 6B). All three *GAL4* elements drove strong GFP fluorescence in the γ MBn and weak expression in the αβ MBn 2 days into pupation. By 4 days into pupation, the GFP expression was strong in both the γ and αβ MBn. This developmental expression pattern analysis is consistent with a requirement for normal MCE in both αβ and γ MBn during pupation for normal ITM in adult flies.

We confirmed these results by measuring 3 hr memory in flies in which *MICU1 RNAi* expression was driven by *201y-GAL4* (Figure S2B) or *R25H11-GAL4* (Figure S2C). We observed a similar decrement in ITM using both drivers. We found no significant difference between control and MCU- or MICU1-silenced flies in odor and shock avoidance assays performed with the αβ and γ-specific drivers (Figure S1B,C,F,G).

Silencing MCU decreases synaptic vesicles in MBn

The developmental requirement for normal MCE to obtain normal ITM in adult flies presented the hypothesis that MCE is involved in the structural or physiological development of MBn necessary to support adult memory. MCU silencing might thus cause a structural change in MBn that is important for ITM. We tested this hypothesis by comparing mCD8::GFP expression in control and MCU-silenced flies. For these experiments we used the *201y-GAL4* driver since it offered the most restricted subset of MBn required for MCE-mediated ITM. A significant difference in the mean average fluorescence intensity between control and experimental group could reflect a change in the number of axonal or dendritic fibers occupying a defined space, or a change in the volume of space occupied by the neuritic fibers.

We stained adult brains with an anti-GFP antibody and measured the mean fluorescence intensity of a ROI that includes the horizontal lobes of the MBn (Figure 7A). The average signal intensity did not differ between control and MCU silenced brains (Figure 7A). We repeated the analysis for the MBn calyx and also found no difference (Figure 7B). The results from these coarse experiments indicate that MCU silencing does not cause a gross structural alteration in MBn neuropil.

We then extended our analyses to assay synaptic vesicle content in the MBn horizontal lobes using as a surrogate the synaptic vesicle marker syt::GFP (Zhang et al., 2002). Silencing MCU caused a significant decrease of the mean syt::GFP fluorescence intensity (Figure 7C), suggesting that MCE impairment reduces synaptic vesicle number and/or size in the horizontal MBn lobes. We also analyzed the dendritic compartment of the MBn using the dendritic marker DenMark (Nicolai et al., 2010). In this case, no difference between control and MCU silenced flies was found (Figure 7D).

To determine whether the decrease in syt::GFP signal was due to an acute decrease in MCE in adult flies but inconsequential to memory, or whether it tracked the developmental requirement for normal MCE for complete ITM, we analyzed syt::GFP staining in flies in which *MCU RNAi* and syt::GFP expression were controlled using the TARGET system. We stained brains in which *MCU RNAi* and syt::GFP were expressed both during development and adulthood (Figure 7E). We confirmed the decrease in syt::GFP mean intensity already shown in Figure 7C without the presence of the *tub-GAL80^{ts}* insertion. However, we failed to detect this difference when the expression of *MCU RNAi* and syt::GFP were activated after eclosion (Figure 7F). The reciprocal temperature shift experiment of activating *MCU RNAi* and syt::GFP expression during development with a downshift at eclosion would not be revealing since the reporter transgene would be shut off during adulthood and therefore undetectable. Altogether, these data show that the decrease in synaptic vesicle reporter expression tracks in broad terms the MCE developmental requirement for normal ITM.

MCU silencing causes an increase of αβ MBn axon length and field volume

Although the data presented above point to an association between pupal stage MCE, ITM and synaptic vesicle number using the syt::GFP as a reporter, we wondered whether there might be other structural changes to the MBn that remained undetectable from these analyses. We thus labeled and analyzed the structure of single MBn using flies expressing a photoactivatable GFP (Ruta et al., 2010) (Figure 7G). We first focused on αβ MBn since they are formed during the same developmental time window during which MCE is required for normal adult ITM (e.g, after pupariation, Lee et al., 1999).

Silencing MCU caused a significant increase in the length of the αβ MBn axons (control: 270±9 μm; MCU RNAi: 329±10 μm; Figure 7H). The number of nodes (junctions) was not statistically different (control: 2.8±0.4 nodes; MCU RNAi: 4.4±0.8 nodes; Figure 7I; p=0.1). We then performed a convex Hull analysis to estimate the volume of the MBn lobe occupied by each photoactivated αβ axon.

With MCU silencing, αβ MBn exhibited an increase in the axonal field volume (control: 40,687±2,813 μm^3; MCU RNAi: 60,126±5,114 μm^3; Figure 7J). Single neuron structural analysis thus demonstrated that MCE is associated with proper control over axonal length and volume. This conclusion was true only for αβ MBn; the same analyses in γ MBn (Figure S3A) failed to show any significant change in axon length, nodes or field volume (Figure S3B-D).

Discussion

The mitochondrial calcium uniporter complex is involved in cellular processes ranging from bioenergetics to apoptosis (Rizzuto et al., 2012). However, our understanding of its roles in neurons *in vivo*, and in particular in cognitive processes such as learning and memory, is poor. In the current study we manipulated the function of the uniporter complex in the *Drosophila* CNS both during development and in the adult animal and related these perturbations to learning and memory. Our results offer four major conclusions: (1) the uniporter is specifically required in αβ γMBn for ITM performance but not for acquisition; (2) it is required during development and not during adulthood at the time of conditioning and testing for flies to display normal ITM; (3) the developmental perturbation that impairs ITM also reduces the synaptic vesicle content in the MBn axons; (4) MCU knockdown does not alter γ MBn structure, but it increases αβ MBn axon length by ~20% and the volume of neuropil occupied by ~50%.

Our findings linking developmental MCE impairment to memory might seem surprising given the report that outbred MCU knockout mice display only a very mild muscle phenotype (Pan et al., 2013). However, the MICU1 knockout is perinatally lethal (Antony et al., 2016) and MCU knockout in a C56BL/6 background is embryonically lethal (Murphy et al., 2014). Consistent with the lethality associated with mouse MCU loss of function, we observed that ubiquitous RNAi-mediated silencing of MCU or MICU1 produces late-pupal lethality. The genetic toolkit that includes RNAi transgenes available to study gene function in *Drosophila* allowed us to circumvent this lethality and map MCE requirement for adult

ITM to the pupal stage of development and to specific populations of neurons (αβ and γ MBn).

It is surprising that genetic insults to MCE during development impair memory in the adult organism without detectably altering acquisition. MCE is a key regulator of many important cellular functions, including coupling of cellular stimulation with ATP production and buffering of cytoplasmic calcium transients (Rizzuto et al., 2012). Because of these real time cellular functions, we had anticipated that the uniporter's role in ITM would be delimited to the adult stage and not to developmental stages that precede conditioning and testing by more than 4 days. One might also anticipate that developmental influences would impact acquisition and memory, rather than specifically affecting memory. However, one caveat of this is that the genetic modifications used in this study produce a partial loss of function and more severe insults might influence acquisition processes. Overall, the results dictate the conclusion that uniporter function in developing MBn establishes the neurons' competence to support adult memory by participating in processes that provide proper neuronal structure, physiology and/or circuitry.

Our single cell photoactivation studies revealed that αβ MBn axons of MCU silenced flies are longer and occupy more neuropil volume. Interestingly, the αβ MBn are born after puparium formation (Lee et al., 1999), coinciding in time with the MCU requirement to support ITM. Like neurons from mammalian species, *Drosophila* MBn undergo activity-dependent refinement in the first few hours after eclosion (Doll and Broadie, 2014; Tessier and Broadie, 2008). Thus, it may be that MCE is required for axonal growth control during pupation or for the activity-dependent refinement of neuronal processes (Tessier and Broadie, 2008). At this stage, the growth control hypothesis seems more likely since a defect in activity-dependent refinement is predicted to cause an increase in short branches only (Tessier and Broadie, 2008). The γ MBn may escape the effect of MCE inhibition through compensatory mechanisms or their axonal retraction/re-extension phase during early pupation (Lee et al., 1999) may be slightly outside of the MCE phenocritical time window. The structural change of αβ neurons is not likely the sole cause of the observed ITM impairment since driving *MCU RNAi* expression specifically in these neurons should have reproduced the ITM decrease observed with combined αβ and γ expression.

The developmental decrease in synaptic vesicle content that we measured with synaptotagmin-GFP expression offers an additional cellular correlate for the ITM phenotype. Numerous studies have linked synaptic release with mitochondrial function (Ivannikov et al., 2013; Sun et al., 2013; Verstreken et al., 2005) and MCU silencing reportedly increases the rate of synaptic vesicle endocytosis (Marland et al., 2016). However, these studies involve acute physiological stimulation. How MCE inhibition during development might translate to an adult deficit in synaptic vesicle content requires further study.

Our discovery of a developmental role for the mitochondrial calcium uniporter complex in regulating ITM in adult flies is particularly interesting since patients carrying loss-of-function mutations in MICU1 display learning difficulties (Lewis-Smith et al., 2016; Logan et al., 2014). Our results measuring a decreased KCl-stimulated calcium entry into

mitochondria with MICU1 deficiency is consistent with the impaired mitochondrial uptake observed by Lewis-Smith et al. (2016) in MICU1-deficient human fibroblasts. However, these results are opposite to the increased rate observed for histamine-stimulated, MICU1-deficient fibroblasts as reported by Logan et al (2014). In light of these discrepancies, it is difficult to draw a strict correlation between MICU1 function, calcium entry into mitochondria, and cognition. Nevertheless, there are many explanations for the observed differences in results, including the type of cellular stimulation used, possible differences in the uniporter complex composition between fibroblasts and neurons, and adaptation mechanisms that might come into play with a complete loss of MICU1 versus a tissue-specific silencing. Additional studies are required to resolve the basis for these differences. Prior studies of genes involved in *Drosophila* olfactory classical conditioning have revealed the utility of the fly in identifying behaviorally relevant genes in humans, although the difference in complexity of the two systems precludes expecting a precise correspondence in phenotypes. As one example, the classic mutant *dunce* in *Drosophila* encodes a cAMP phosphodiesterase and its disruption impairs olfactory learning after classical conditioning (Davis, 2005) while the human homologs of dunce are involved in mood regulation and psychiatric disorders (Henkel-Tigges and Davis, 1990; Millar et al., 2005). Our study thus offers guidance in further pursuit of understanding mitochondrial uniporter function, neuronal development, and adult cognition.

Experimental Procedures

Fly stocks and behavior

Fly stocks were raised on standard food at room temperature. Supplementary Table 1 lists the stocks used in this study. Fly crosses were maintained at 25C with ~70% relative humidity on a 12 hr light:12 hr dark cycle. For olfactory aversive conditioning, experiments were performed as already described (Walkinshaw et al., 2015). Additional details are available in the Supplementary experimental procedures.

Functional mitochondrial calcium imaging

Brains from 5 day-old flies were dissected and perfused with a saline solution (124 mM NaCl, 3 mM KCl, 20 mM MOPS, 1.5 mM $CaCl_2$, 4 mM $MgCl_2$, 5 mM $NaHCO_3$, 1mM NaH_2PO_4, 10 mM trehalose, 7 mM sucrose, 10 mM glucose; pH 7.2 at 25C). KCl stimulation was performed by perfusing brains with the appropriate concentration of KCl made in saline solution. Additional details are available in the Supplementary experimental procedures.

Immunohistochemistry and image analysis

For all immunohistochemistry experiments, we followed the protocol described by Jenett et al. (2012). Additional details are available in the Supplementary experimental procedures.

Single neuron structural analyses

Photoactivation experiments were performed using a Leica TCS SP8 confocal microscope equipped with a Chameleon™ Vision S Ti:S laser (Coherent) tuned at 710 nm. Five day-old fly brains were dissected and positioned in a chamber filled with saline (above). The cell

body of a single MBn was identified using a 25X water immersion objective. An ROI of 1 μm diameter was designated at the center of the cell body and C3PA-GFP was photoactivated by the 710 nm Ti:S laser. The photoactivation protocol consisted of 3 line scans of the ROI followed by a 2 min pause to allow GFP diffusion. This protocol was repeated 30 times. The Ti:S laser power was adjusted to an output power of 20 to 40 mW measured at the objective. After photoactivation, the MBn axonal projections were imaged using a 63X objective and a 488 nm Argon laser. Total neuron length and the number of nodes were measured using the 'Branched structure analysis' function of Neurolucida Explorer (MBF Bioscience) while field volume of axonal projections was calculated using the 'Convex Hull analysis' function.

Statistical analyses

Statistical analyses were performed using GraphPad Prism. Memory scores follow a normal distribution (Walkinshaw et al., 2015) and were thus analyzed by two-tailed, two-sample Student's t-test. For multiple group comparisons, we used one-way or two-way ANOVA followed by Bonferroni's multiple comparison test. Dunnett's multiple comparison test was used when multiple groups were compared to the same control. For experiments other than behavioral, we first assessed normality of the data using the D'Agostino & Pearson test. The Mann-Whitney test was used when the assumption of normality was not possible.

Supplementary Material

Refer to Web version on PubMed Central for supplementary material.

Acknowledgments

We thank Richard Axel, Tullio Pozzan, Rosario Rizzuto, VDRC and Bloomington for reagents. We are grateful to Massimiliano Aceti for advice provided about use of Neurolucida software. This research was supported by NIH grants R37NS19904 and R01NS052351 to RD. We are grateful to the Iris and Junming Le Foundation for funds to purchase a super-resolution microscope.

References

Antony AN, Paillard M, Moffat C, Juskeviciute E, Correnti J, Bolon B, Rubin E, Csordas G, Seifert EL, Hoek JB, et al. MICU1 regulation of mitochondrial Ca^{2+} uptake dictates survival and tissue regeneration. Nat. Commun. 2016; 7:10955. [PubMed: 26956930]

Baughman JM, Perocchi F, Girgis HS, Plovanich M, Belcher-Timme CA, Sancak Y, Bao XR, Strittmatter L, Goldberger O, Bogorad RL, et al. Integrative genomics identifies MCU as an essential component of the mitochondrial calcium uniporter. Nature. 2011; 476:341–345. [PubMed: 21685886]

Csordas G, Golenar T, Seifert EL, Kamer KJ, Sancak Y, Perocchi F, Moffat C, Weaver D, de la Fuente Perez S, Bogorad R, et al. MICU1 controls both the threshold and cooperative activation of the mitochondrial Ca^{2+} uniporter. Cell metab. 2013; 17:976–987. [PubMed: 23747253]

Davis RL. Olfactory memory formation in Drosophila: from molecular to systems neuroscience. Annu. Rev. Neurosci. 2005; 28:275–302. [PubMed: 16022597]

De Stefani D, Raffaello A, Teardo E, Szabo I, Rizzuto R. A forty-kilodalton protein of the inner membrane is the mitochondrial calcium uniporter. Nature. 2011; 476:336–340. [PubMed: 21685888]

Doll CA, Broadie K. Impaired activity-dependent neural circuit assembly and refinement in autism spectrum disorder genetic models. Front. Cell. Neurosci. 2014; 8:30. [PubMed: 24570656]

Finsterer J. Cognitive dysfunction in mitochondrial disorders. Acta neurol. Scand. 2012; 126:1–11. [PubMed: 22335339]

Guven-Ozkan T, Davis RL. Functional neuroanatomy of Drosophila olfactory memory formation. Learn. Mem. 2014; 21:519–526. [PubMed: 25225297]

Hara Y, Yuk F, Puri R, Janssen WG, Rapp PR, Morrison JH. Presynaptic mitochondrial morphology in monkey prefrontal cortex correlates with working memory and is improved with estrogen treatment. Proc. Natl. Acad. Sci. USA. 2014; 111:486–491. [PubMed: 24297907]

Hara Y, Yuk F, Puri R, Janssen WG, Rapp PR, Morrison JH. Estrogen restores multisynaptic boutons in the dorsolateral prefrontal cortex while promoting working memory in aged rhesus monkeys. J. Neurosci. 2016; 36:901–910. [PubMed: 26791219]

Henkel-Tigges J, Davis RL. Rat homologs of the Drosophila dunce gene code for cyclic AMP phosphodiesterases sensitive to rolipram and RO 20-1724. Mol. Pharmacol. 1990; 37:7–10. [PubMed: 2153912]

Ivannikov MV, Sugimori M, Llinas RR. Synaptic vesicle exocytosis in hippocampal synaptosomes correlates directly with total mitochondrial volume. J. Mol. Neurosci. 2013; 49:223–230. [PubMed: 22772899]

Jenett A, Rubin GM, Ngo TT, Shepherd D, Murphy C, Dionne H, Pfeiffer BD, Cavallaro A, Hall D, Jeter J, et al. A GAL4-driver line resource for Drosophila neurobiology. Cell Rep. 2012; 2:991–1001. [PubMed: 23063364]

Kamer KJ, Mootha VK. MICU1 and MICU2 play nonredundant roles in the regulation of the mitochondrial calcium uniporter. EMBO Rep. 2014; 15:299–307. [PubMed: 24503055]

Kamer KJ, Mootha VK. The molecular era of the mitochondrial calcium uniporter. Nat. Rev. Mol. Cell Biol. 2015; 16:545–553. [PubMed: 26285678]

Lee T, Lee A, Luo L. Development of the Drosophila mushroom bodies: sequential generation of three distinct types of neurons from a neuroblast. Development. 1999; 126:4065–4076. [PubMed: 10457015]

Lewis-Smith D, Kamer KJ, Griffin H, Childs AM, Pysden K, Titov D, Duff J, Pyle A, Taylor RW, Yu-Wai-Man P, et al. Homozygous deletion in MICU1 presenting with fatigue and lethargy in childhood. Neurol. Genet. 2016; 2:e59. [PubMed: 27123478]

Logan CV, Szabadkai G, Sharpe JA, Parry DA, Torelli S, Childs AM, Kriek M, Phadke R, Johnson CA, Roberts NY, et al. Loss-of-function mutations in MICU1 cause a brain and muscle disorder linked to primary alterations in mitochondrial calcium signaling. Nat. Genet. 2014; 46:188–193. [PubMed: 24336167]

Lye CM, Naylor HW, Sanson B. Subcellular localisations of the CPTI collection of YFP-tagged proteins in Drosophila embryos. Development. 2014; 141:4006–4017. [PubMed: 25294944]

Marland JR, Hasel P, Bonnycastle K, Cousin MA. Mitochondrial calcium uptake modulates synaptic vesicle endocytosis in central nerve terminals. J. Biol. Chem. 2016; 291:2080–2086. [PubMed: 26644474]

McGuire SE, Le PT, Osborn AJ, Matsumoto K, Davis RL. Spatiotemporal rescue of memory dysfunction in Drosophila. Science. 2003; 302:1765–1768. [PubMed: 14657498]

Millar JK, Pickard BS, Mackie S, James R, Christie S, Buchanan SR, Malloy MP, Chubb JE, Huston E, Baillie GS, et al. DISC1 and PDE4B are interacting genetic factors in schizophrenia that regulate cAMP signaling. Science. 2005; 310:1187–1191. [PubMed: 16293762]

Murphy E, Pan X, Nguyen T, Liu J, Holmstrom KM, Finkel T. Unresolved questions from the analysis of mice lacking MCU expression. Biochem. Biophys. Res. Commun. 2014; 449:384–385. [PubMed: 24792186]

Nicolai LJ, Ramaekers A, Raemaekers T, Drozdzecki A, Mauss AS, Yan J, Landgraf M, Annaert W, Hassan BA. Genetically encoded dendritic marker sheds light on neuronal connectivity in Drosophila. Proc. Natl. Acad. Sci. USA. 2010; 107:20553–20558. [PubMed: 21059961]

Oxenoid K, Dong Y, Cao C, Cui T, Sancak Y, Markhard AL, Grabarek Z, Kong L, Liu Z, Ouyang B, et al. Architecture of the mitochondrial calcium uniporter. Nature. 2016; 533:269–273. [PubMed: 27135929]

Pan X, Liu J, Nguyen T, Liu C, Sun J, Teng Y, Fergusson MM, Rovira II, Allen M, Springer DA, et al. The physiological role of mitochondrial calcium revealed by mice lacking the mitochondrial calcium uniporter. Nat. Cell Biol. 2013; 15:1464–1472. [PubMed: 24212091]

Patron M, Checchetto V, Raffaello A, Teardo E, Vecellio Reane D, Mantoan M, Granatiero V, Szabo I, De Stefani D, Rizzuto R. MICU1 and MICU2 finely tune the mitochondrial Ca^{2+} uniporter by exerting opposite effects on MCU activity. Mol. Cell. 2014; 53:726–737. [PubMed: 24560927]

Perocchi F, Gohil VM, Girgis HS, Bao XR, McCombs JE, Palmer AE, Mootha VK. MICU1 encodes a mitochondrial EF hand protein required for Ca^{2+} uptake. Nature. 2010; 467:291–296. [PubMed: 20693986]

Plovanich M, Bogorad RL, Sancak Y, Kamer KJ, Strittmatter L, Li AA, Girgis HS, Kuchimanchi S, De Groot J, Speciner L, et al. MICU2, a paralog of MICU1, resides within the mitochondrial uniporter complex to regulate calcium handling. PloS one. 2013; 8:e55785. [PubMed: 23409044]

Rizzuto R, De Stefani D, Raffaello A, Mammucari C. Mitochondria as sensors and regulators of calcium signalling. Nat. Rev. Mol. Cell Biol. 2012; 13:566–578. [PubMed: 22850819]

Ruta V, Datta SR, Vasconcelos ML, Freeland J, Looger LL, Axel R. A dimorphic pheromone circuit in Drosophila from sensory input to descending output. Nature. 2010; 468:686–690. [PubMed: 21124455]

Sancak Y, Markhard AL, Kitami T, Kovacs-Bogdan E, Kamer KJ, Udeshi ND, Carr SA, Chaudhuri D, Clapham DE, Li AA, et al. EMRE is an essential component of the mitochondrial calcium uniporter complex. Science. 2013; 342:1379–1382. [PubMed: 24231807]

Schon EA, Przedborski S. Mitochondria: the next (neurode)generation. Neuron. 2011; 70:1033–1053. [PubMed: 21689593]

Sun T, Qiao H, Pan PY, Chen Y, Sheng ZH. Motile axonal mitochondria contribute to the variability of presynaptic strength. Cell Rep. 2013; 4:413–419. [PubMed: 23891000]

Tessier CR, Broadie K. Drosophila fragile X mental retardation protein developmentally regulates activity-dependent axon pruning. Development. 2008; 135:1547–1557. [PubMed: 18321984]

Verstreken P, Ly CV, Venken KJ, Koh TW, Zhou Y, Bellen HJ. Synaptic mitochondria are critical for mobilization of reserve pool vesicles at Drosophila neuromuscular junctions. Neuron. 2005; 47:365–378. [PubMed: 16055061]

Walkinshaw E, Gai Y, Farkas C, Richter D, Nicholas E, Keleman K, Davis RL. Identification of genes that promote or inhibit olfactory memory formation in Drosophila. Genetics. 2015; 199:1173–1182. [PubMed: 25644700]

Zhang YQ, Rodesch CK, Broadie K. Living synaptic vesicle marker: synaptotagmin-GFP. Genesis. 2002; 34:142–145. [PubMed: 12324970]

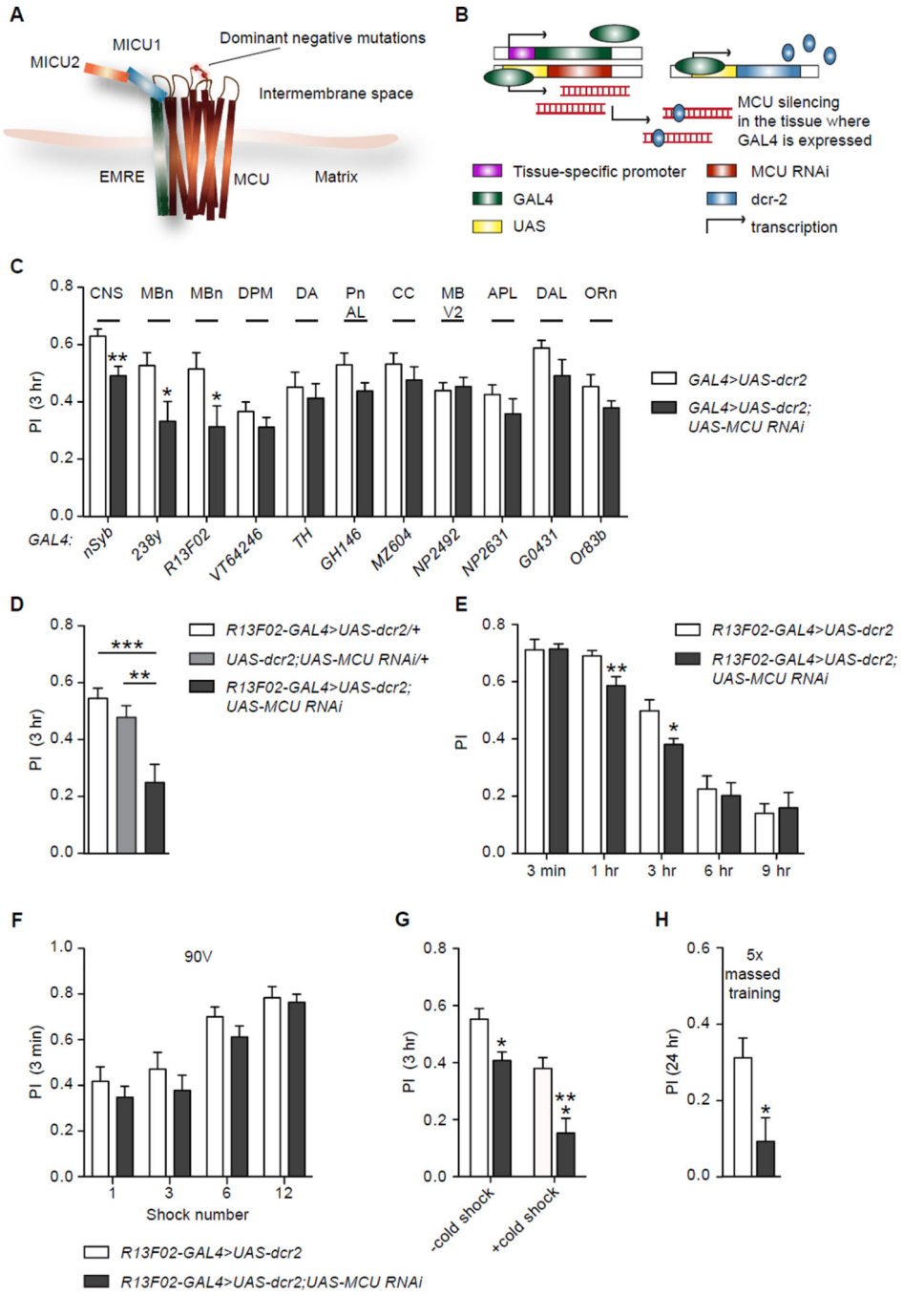

Figure 1. Silencing MCU in MBn impairs olfactory memory without altering learning

(A) Schematic representation of the mitochondrial calcium uniporter complex including MCU, EMRE, MICU1 and MICU2. Other components of the channel are omitted for simplicity. The complex is situated in the inner mitochondrial membrane to mediate calcium import from the intermembrane space into the matrix. The amino acids of MCU that, when mutated, produce a dominant negative form are identified as red dots.

(B) Schematic diagram of the three transgenes used to silence MCU in a tissue-specific manner. One transgene carries *GAL4* transcription activator sequences under the control of a

tissue specific promoter. The GAL4 protein is expressed in a tissue-specific way, driving the transcription of *MCU RNAi* and *dicer-2* (*dcr-2*) mRNA by binding to Upstream Activating Sequences (UAS elements) carried on the two other transgenes. Dicer-2 expression enhances the effect of the RNAi.

(C) MCU silencing in MBn impaired memory. *UAS-dcr2* or *UAS-dcr2;MCU RNAi* flies were crossed to a battery of *GAL4* lines that drive expression of *UAS*-transgenes in specific populations of neurons. CNS, central nervous system; MBn, mushroom body neurons; DPM, dorsal paired medial neurons; DA, dopaminergic neurons; Pn AL, projection neurons of the antennal lobe; CC, central complex; MB V2, mushroom body V2 output neurons; APL, anterior paired lateral neurons; DAL, dorsal anterior lateral neurons; ORn, olfactory receptor neurons. Silencing MCU in MBn using *238y-* or *R13F02-GAL4* impaired 3 hr olfactory memory. PI=Performance Index (*$p<0.05$). The *nSyb-GAL4* pan-neuronal driver was used as a positive control (**$p<0.01$). Results are expressed as the mean ± SEM with $n\geq8$ and were analyzed by two-tailed, two-sample Student's t-tests.

(D) MCU silencing in MBn impaired 3 hr memory relative to two independent genetic controls: flies that are heterozygous either for the *R13F02-GAL4* insertion or the *UAS-MCU RNAi* insertion. PIs are expressed as the mean ± SEM with n=12 and were analyzed by one-way ANOVA followed by Bonferroni post hoc tests (** $p<0.01$; *** $p<0.001$).

(E) Silencing MCU in MBn did not affect immediate memory (3 min) but decreased ITM (1 hr: **$p<0.01$; 3 hr: *$p<0.05$). PIs are expressed as the mean ± SEM with $n\geq8$ and each time point was analyzed by two-tailed, two-sample Student's t-test.

(F) Silencing MCU in MBn did not impair memory acquisition. Three min PIs were measured after training with 1, 3, 6 or 12 electric shock pulses at 90V. PIs are expressed as the mean ± SEM with n=6 and were analyzed by two-tailed, two-sample Student's t-tests.

(G) Silencing MCU in MBn impairs ARM. PIs are expressed as the mean ± SEM with n=14 and were analyzed by two-way ANOVA followed by Bonferroni post hoc tests (−cold shock: *$p<0.05$; +cold shock: ***$p<0.001$).

(H) Silencing MCU in MBn impaired memory after 5X massed training. PIs are expressed as the mean ± SEM with n=14 and were analyzed by two-tailed, two-sample Student's t-tests (*$p<0.05$).

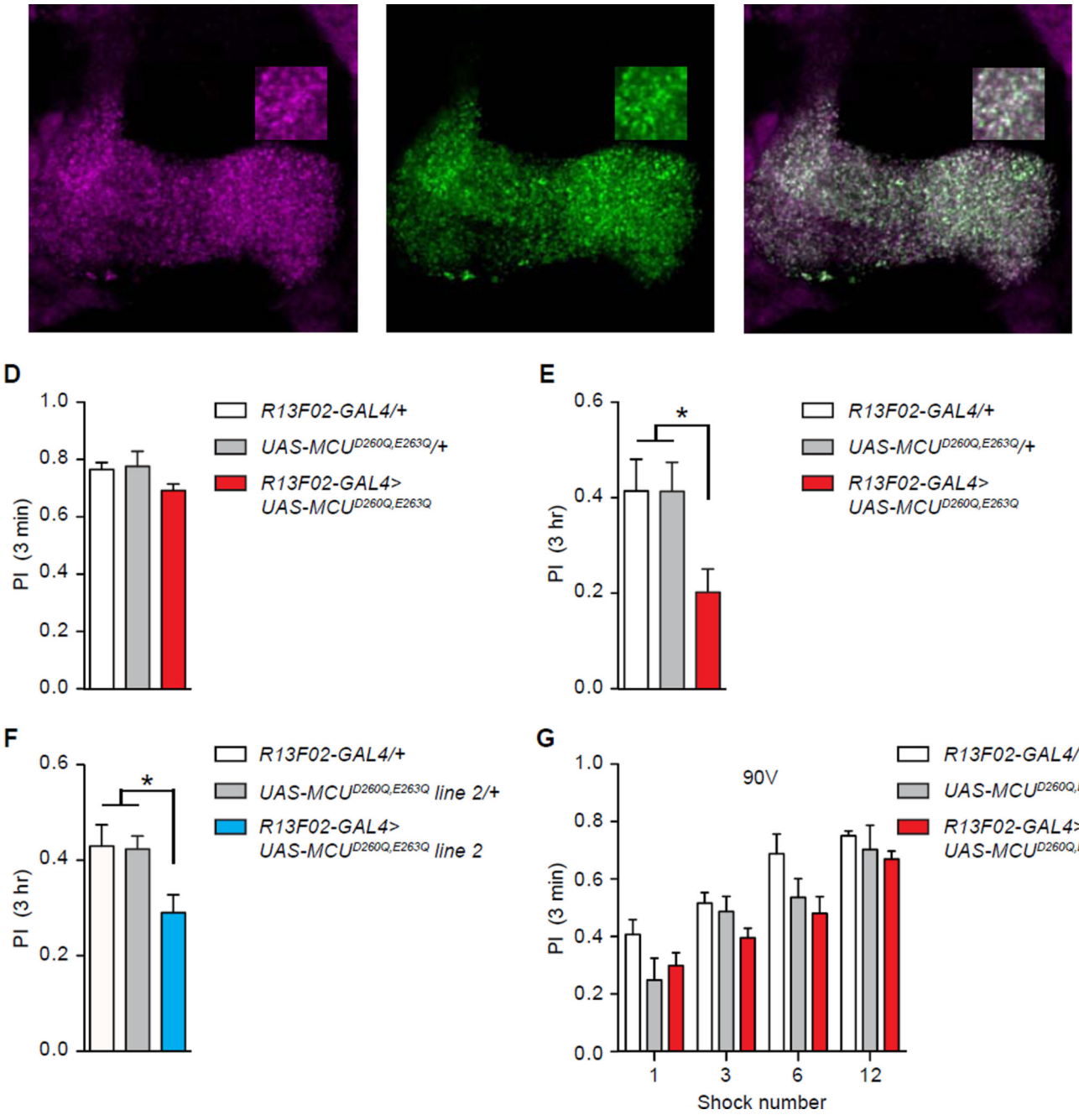

Figure 2. Expressing a dominant negative form of MCU (MCU^{D260Q,E263Q}) in MBn impairs olfactory memory without altering learning

(A-C) The expression of MCU^{D260Q,E263Q} in MBn was detected with an anti-FLAG antibody (A, magenta), while mito-GFP expression was detected with an anti-GFP antibody (B, green). (C) Merged image of (A) and (B) showing the co-localization of the MCU^{D260Q,E263Q} signal with mito-GFP in a single confocal section of MBn horizontal lobe. The insets for each panel illustrate a magnified view of the selected region for better visualization of the coincidental signals. Scale bar, 10 μm.

(D) Expression of $MCU^{D260Q,E263Q}$ in MBn did not impair immediate memory. Results are expressed as the mean ± SEM with n=8 and were analyzed by one-way ANOVA followed by Bonferroni post hoc tests.
(E) Expression of $MCU^{D260Q,E263Q}$ in MBn decreased 3 hr memory (*$p<0.05$). PIs are expressed as the mean ± SEM with n=10 and were analyzed by one-way ANOVA followed by Bonferroni post hoc tests.
(F) Expression of $MCU^{D260Q,E263Q}$ in MBn using a second insertion line decreased 3 hr memory (*$p<0.05$). PIs are expressed as the mean ± SEM with n=12 and were analyzed by one-way ANOVA followed by Bonferroni post hoc tests.
(G) $MCU^{D260Q,E263Q}$ expression in MBn did not affect memory acquisition. PIs are expressed as the mean ± SEM with n=6 and were analyzed by one-way ANOVA between genotypes for each shock condition.

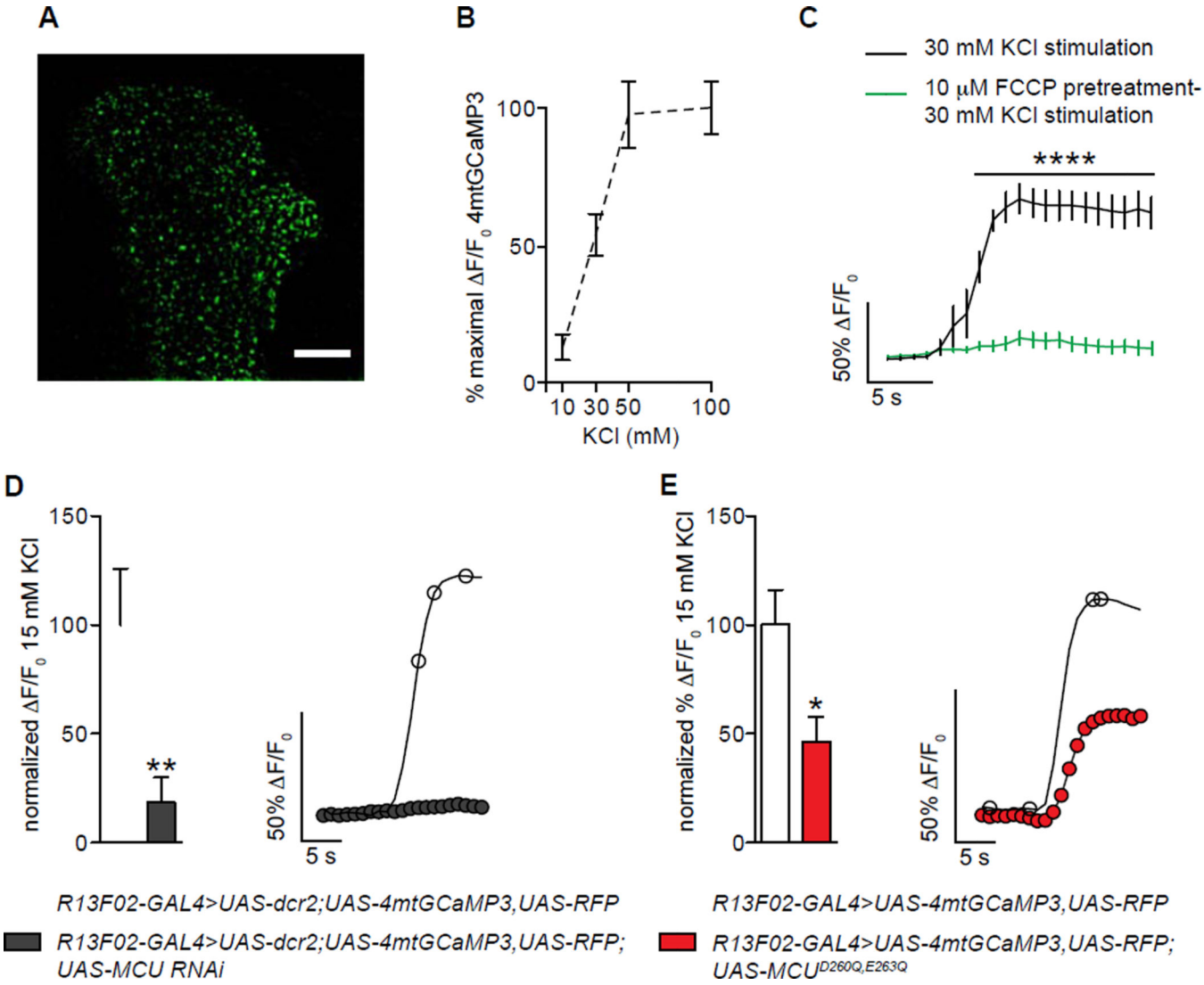

Figure 3. Impairing MCU function in MBn decreases MCE

(A) Image of the tip of MBn vertical lobe obtained using structured illumination microscopy. The 4mtGCaMP3 reporter was expressed using *R13F02-GAL4*. Scale bar, 5 μm.

(B) Dose-response curve of the 4mtGCaMP3 mitochondrial calcium reporter. Brains from *OK107-GAL4>UAS-4mtGCaMP3* flies were isolated and stimulated with 10, 30, 50 or 100 mM KCl. The 100 mM KCl response was taken as maximal and normalized as 100%. The $\Delta F/F_0$ peak responses are expressed as the percentage of the maximal $\Delta F/F_0 \pm$ SEM with $n \geq 6$.

(C) The 4mtGCaMP3 reporter localizes to the mitochondrial matrix. The signal increase of 4mtGCaMP3 upon 30 mM KCl stimulation (black) was abolished by pretreatment with the mitochondrial uncoupler FCCP (green). The traces represent the mean $\%\Delta F/F_0 \pm$ SEM at each time point after stimulation with n=5. Single traces were compared by two-way ANOVA with repeated measures followed by Bonferroni post hoc tests (****$p<0.0001$).

(D) Silencing MCU in MBn decreased MCE in isolated brains (**$p<0.01$). The 15 mM KCl peak responses of controls were normalized to 100%; responses of the MCU silenced group

are expressed as the mean of the normalized $\Delta F/F_0 \pm$ SEM ($n \geq 11$). They were analyzed by two-tailed, two-sample Student's t-test. Representative individual traces of a control (open circles) and a MCU silenced brain (black circles) are shown at the right.

(E) $MCU^{D260Q,E263Q}$ expression in MBn decreased MCE in isolated brains (*$p<0.05$). The 15 mM KCl peak responses of controls were normalized to 100%; responses of the $MCU^{D260Q,E263Q}$ group are expressed as the mean of the normalized $\Delta F/F_0 \pm$ SEM ($n \geq 10$). They were analyzed by two-tailed, two-sample Student's t-test. Representative individual traces of a control (open circles) and $MCU^{D260Q,E263Q}$ expressing brain (red circles) are shown at the right.

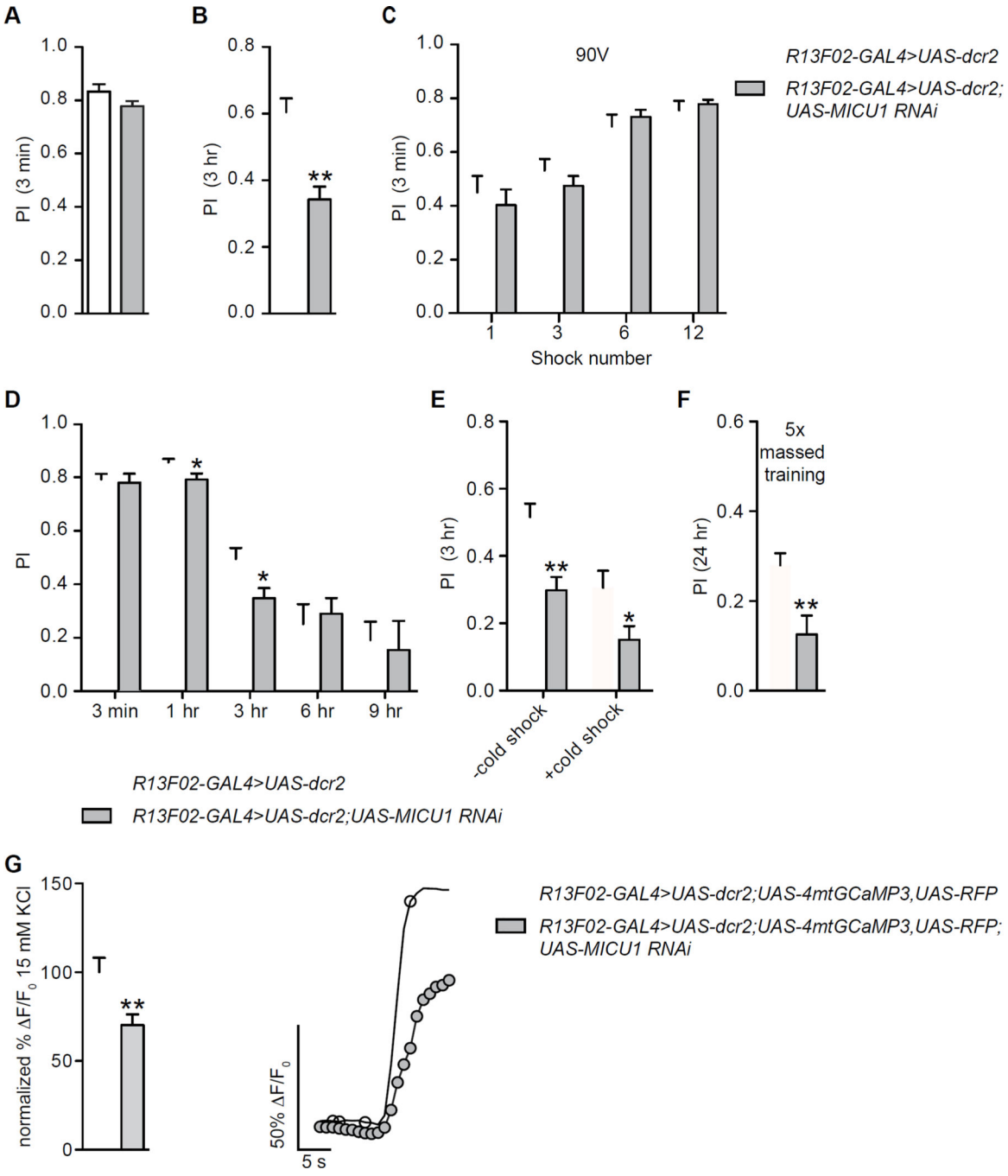

Figure 4. Silencing MICU1 in MBn recapitulates the memory impairment caused by MCU silencing

(A) Silencing MICU1 in MBn did not alter immediate memory. PIs are expressed as the mean ± SEM with n=8 and were analyzed by two-tailed, two-sample Student's t-tests.

(B) Silencing MICU1 in MBn decreased 3 hr memory (**p<0.01). PIs are expressed as the mean ± SEM with n=14 and were analyzed by two-tailed, two-sample Student's t-tests.

(C) Silencing MICU1 in MBn did not alter memory acquisition. PIs are expressed as the mean ± SEM with n=6 and were analyzed by two-tailed, two-sample Student's t-tests.

(D) Silencing MICU1 in MBn decreased ITM (1 hr and 3 hr; *p<0.05). PIs are expressed as the mean ± SEM with n=8 and each time point was analyzed by two-tailed, two-sample Student's t-test.

(E) Silencing MICU1 in MBn impaired ARM. PIs are expressed as the mean ± SEM with n=12 and were compared using a two-way ANOVA followed by Bonferroni post hoc tests (−cold shock: **p<0.01; +cold shock: *p<0.05).

(F) Silencing MICU1 in MBn impaired memory after 5X massed training. PIs are expressed as the mean ± SEM with n=12 and were analyzed by two-tailed, two-sample Student's t-tests (**p<0.01).

(G) Silencing MICU1 in MBn decreased MCE in isolated brains (**p<0.01). The 15 mM KCl peak responses of controls were normalized to 100%; responses of the MICU1 silenced group are expressed as the normalized $\Delta F/F_0$ ± SEM with n=14 and were analyzed by two-tailed, two-sample Student's t-test. Representative individual traces of a control (open circles) and MICU1 silenced brain (gray circles) are shown at the right.

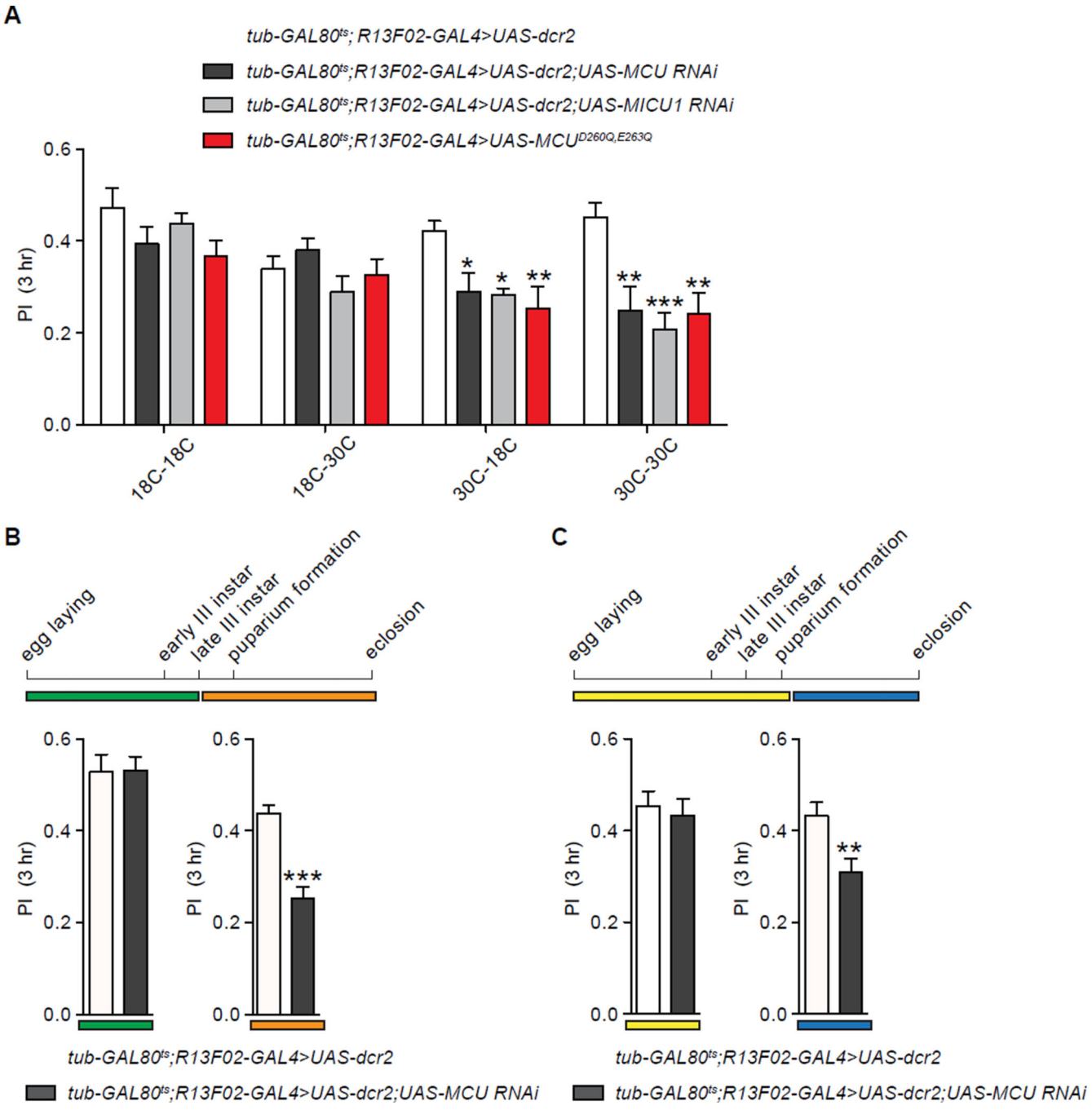

Figure 5. MCE is required in MBn during pupation to support olfactory memory in adult flies

The GAL80^{ts} protein inhibits GAL4 protein activity at 18C but not 30C, thus allowing experimenter-control over the expression of *UAS-MCU RNAi, UAS-MICU1 RNAi* or *UAS-MCU^{D260Q,E263Q}* using temperature shifts at specific time periods during development or adulthood.

(A) Silencing MCU or MICU1, or expressing MCU^{D260Q,E263Q} only during development (30C-18C) produced a 3 hr memory impairment similar to that observed upon silencing MCU or MICU1, or expressing MCU^{D260Q,E263Q}, across development and into adulthood

(30C-30C condition). PIs are expressed as the mean ± SEM with n≥8 and they were analyzed by one-way ANOVA followed by Dunnett's multiple comparison test (* $p<0.05$; ** $p<0.01$; *** $p<0.001$).

(B) Silencing MCU from egg laying until late third instar was not sufficient to produce a memory impairment in adult flies (green bar), while silencing MCU from late third instar to eclosion was sufficient to produce 3 hr memory impairment (orange bar) (*** $p<0.001$). PIs are expressed as the mean ± SEM with n≥12 and they were analyzed by two-tailed, two-sample Student's t-tests.

(C) Silencing MCU from egg laying up the end of puparium formation failed to cause a memory impairment in adult flies (yellow bar), while silencing MCU from the end of puparium formation to eclosion was sufficient to produce the impairment (blue bar), thus mapping MCU function to pupation. PIs are expressed as the mean ± SEM with n≥12 and they were analyzed by two-tailed, two-sample Student's t-tests (** $p<0.01$).

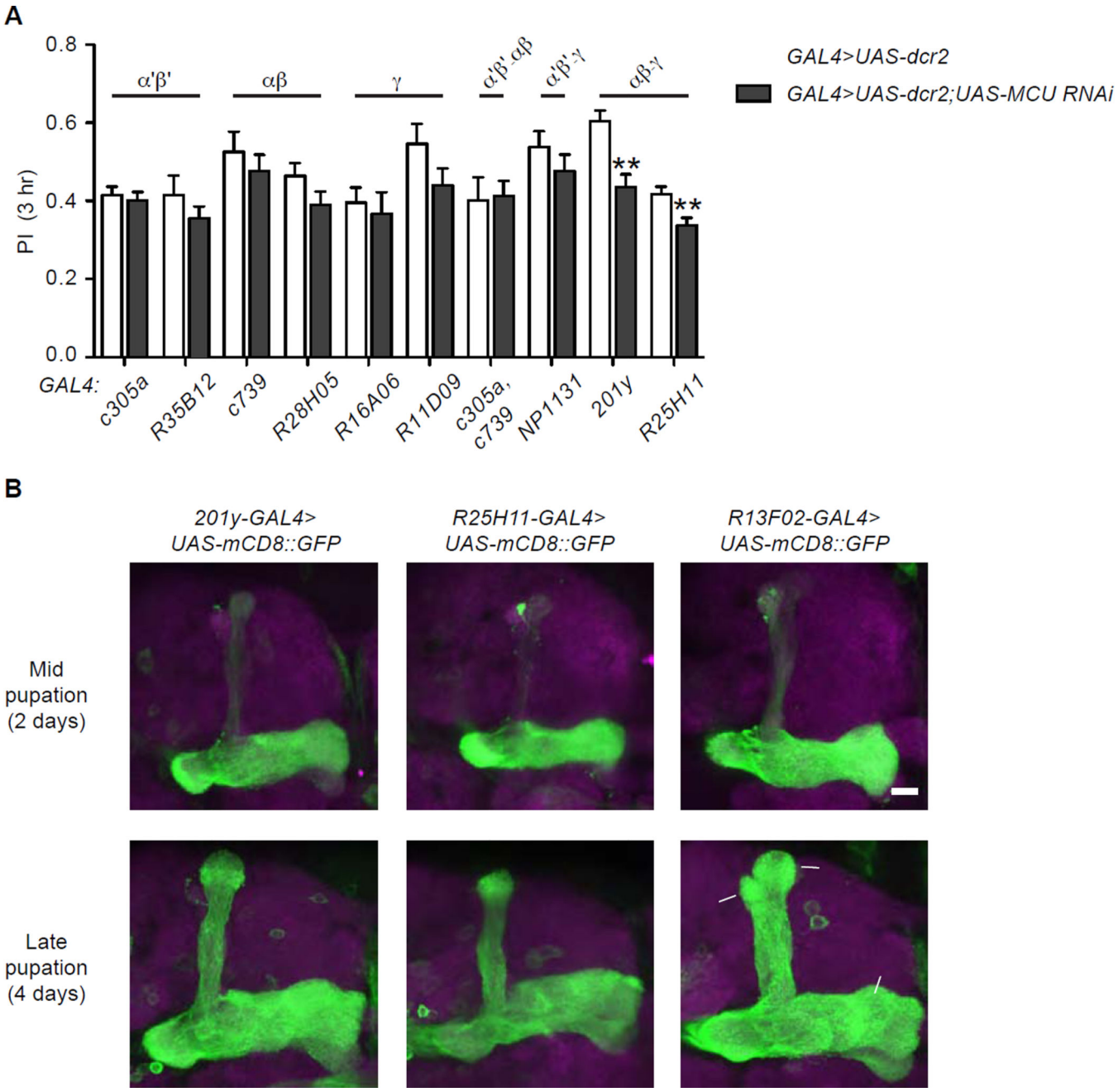

Figure 6. MCU silencing in αβ and γ MBn decreases olfactory memory

(A) *MCU RNAi* was expressed using a panel of *GAL4* drivers that promote expression in single classes of MBn (α'β', αβ or γ) or in a combination of two classes. Only *GAL4* drivers that promote expression of the *RNAi* in both αβ and γ MBn decreased 3 hr memory (**p<0.001). Results are expressed as the mean ± SEM with n≥8 and were analyzed by two-tailed, two-sample Student's t-tests.

(B) Expression pattern of *201y-, R25H11-* and *R13F02-GAL4* in the MBn lobes at two times during pupation. The *UAS-mCD8::GFP* flies were crossed with the indicated *GAL4* and brains from pupae at mid pupation or late pupation were dissected and stained with anti-

GFP (green) and anti-nc82 (magenta) antibodies. Arrows in the late pupation image of *R13F02-GAL4> UAS-mCD8::GFP* identify the α, αβ and γ lobes. The β' and β collaterals of the α'β' and αβ MBn reside more posterior (beneath in this image) and are obscured by the γ lobe neuropil.

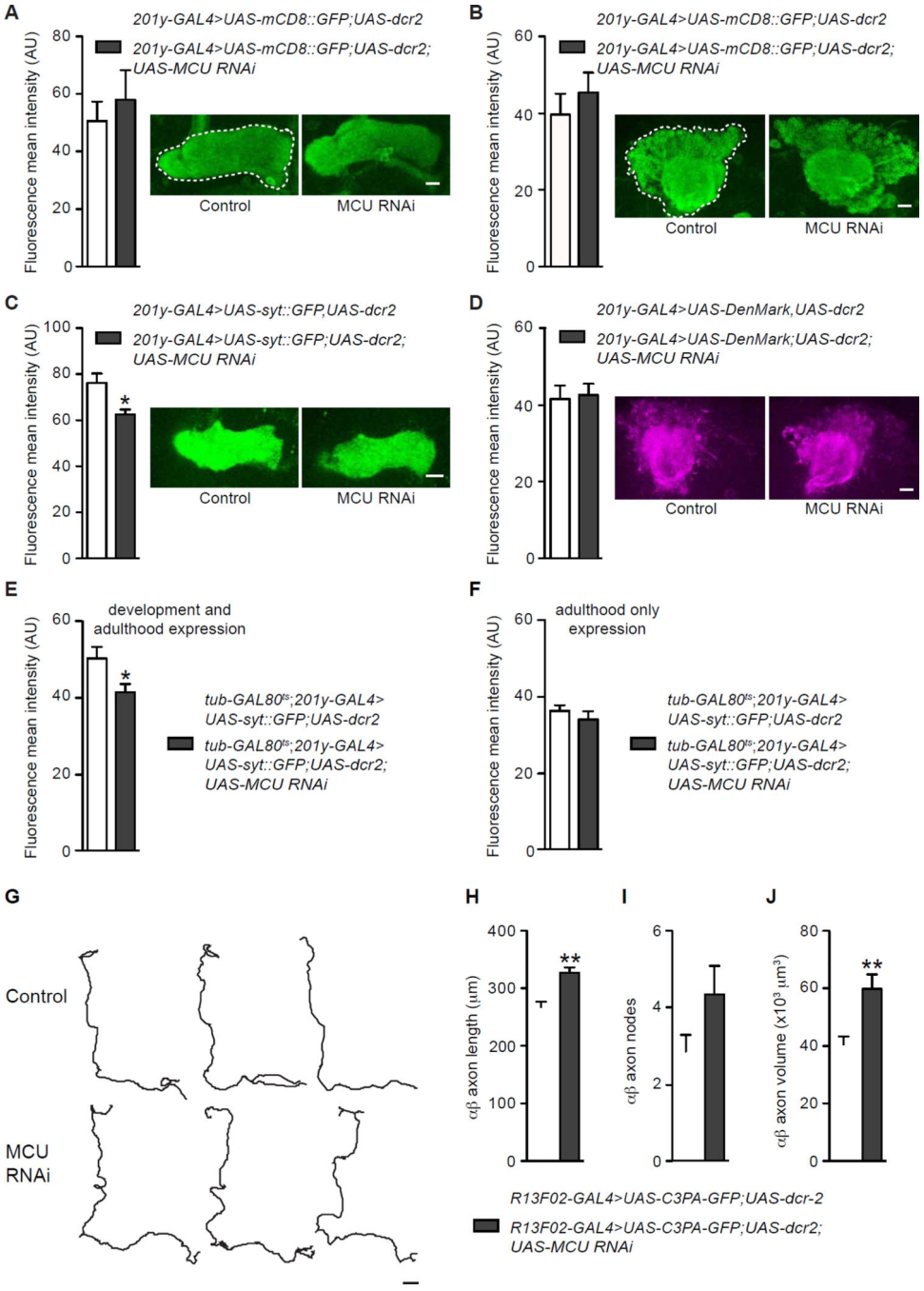

Figure 7. MCU silencing causes a decrease in MBn synaptic vesicle content and an increase of αβ MBn axon length and field volume

(A) Silencing MCU did not alter the mean fluorescence intensity of the MBn horizontal lobes obtained by expressing mCD8::GFP with *201y-GAL4*. For each panel, the bar graph illustrates group data while representative maximal projection images of a control and *MCU RNAi* Z-stack are shown on the right. The dotted line identifies the ROI designed for horizontal lobe analysis. Mean fluorescence intensity is expressed as the mean ± SEM with n=8. Comparisons were made using a two-tailed, two-sample Student's t-test. Scale bar, 10 μm.

(B) Silencing MCU did not alter the mean fluorescence intensity of MBn calyces obtained by expressing mCD8::GFP with *201y-GAL4*. The dotted line identifies the ROI designed for calyx analysis. Mean fluorescence intensity is expressed as the mean ± SEM with n=8. Comparisons were made using a two-tailed, two-sample Student's t-test. Scale bar, 10 μm.
(C) Silencing MCU decreased the mean signal intensity of the synaptic vesicle reporter syt::GFP. Mean fluorescence intensity is expressed as the mean ± SEM with n=8. Comparisons were made using a two-tailed, two-sample Student's t-test (*$p<0.05$). Scale bar, 10 μm.
(D) MCU silencing failed to cause a significant change in the dendritic compartment using DenMark mean fluorescence intensity as a reporter. Mean fluorescence intensity is expressed as the mean ± SEM with n=8. Comparisons were made using a two-tailed, two-sample Student's t-test. Scale bar, 10 μm.
(E) MCU silencing across development and adulthood using the TARGET system produced a significant decrease in the mean intensity of syt::GFP fluorescence. Mean fluorescence intensity is expressed as the mean ± SEM with n=8. Comparisons were made using a two-tailed, two-sample Student's t-test (*$p<0.05$).
(F) MCU silencing during adulthood only using the TARGET system did not produce a significant decrease in the mean intensity of syt::GFP fluorescence. Mean fluorescence intensity is expressed as the mean ± SEM with n=8. Comparisons were made using a two-tailed, two-sample Student's t-test. The combined data suggest that the decrease observed in panel E occurs from MCU silencing during development.
(G) Images of 3 representative control (top) and MCU silenced (bottom) αβ MBn traced with Neurolucida Explorer after C3PA-GFP photoactivation. Scale bar, 10 μm.
(H) Silencing MCU increased the length of αβ MBn axons (**$p<0.01$). Neuron length is expressed as the mean ± SEM with n=8 and was compared by a Mann-Whitney test.
(I) Silencing MCU in MBn did not significantly change the number of αβ MBn nodes. Neuron nodes are expressed as the mean ± SEM with n=8 and they were compared by a Mann-Whitney test.
(J) Silencing MCU increased the volume occupied by the axon branches of αβ MBn (**$p<0.01$) as calculated with convex Hull analysis. Axonal field volumes are expressed as the mean ± SEM with n=8 and they were compared by a Mann-Whitney test.